

煤灰中 Fe₂O₃ 含量对卫燃带表面结渣的影响

陈冬林 杜 洋 陈文卫 焦学鹏

(长沙理工大学 能源与动力工程学院 湖南 长沙 410076)

摘 要: 以冷水江页岩煤灰为基灰,向其添加不同质量的 Fe₂O₃ 粉末,制成 Fe₂O₃ 含量分别为 1.53%、10%、20%、30% 和 40% 煤灰试样若干。首先采用角锥法测量 Fe₂O₃ 含量变化对煤灰熔融特性的影响,然后将不同 Fe₂O₃ 含量煤灰均匀疏松的敷设在碳化硅、高铝刚玉、中铝刚玉 3 种卫燃带耐火材料板表面,并将其置入高温马弗炉内于 1 330℃ 下煅烧 40 h,待煅烧完成后,观察 3 种卫燃带耐火材料板表面的结渣特性,并对灰渣进行 X 射线衍射分析。试验结果表明: 随煤灰中 Fe₂O₃ 含量的增加,煤灰熔融温度均呈下降趋势,同时在卫燃带耐火材料板表面结渣程度均趋于严重,但当煤灰中 Fe₂O₃ 含量增至一定值后,其熔融温度反而呈上升趋势,且在卫燃带耐火材料板表面结渣程度将不再继续增强,反而有所降低。

关 键 词: 煤灰; 卫燃带; 熔融特性; 结渣; Fe₂O₃ 粉末

中图分类号: TQ022; O242 文献标识码: A

引 言

目前,国内外燃用无烟煤、贫煤等低挥发分煤的锅炉几乎都采用基于耐火隔热材料的卫燃带稳燃技术^[1-3]。虽然卫燃带可以显著提高燃煤锅炉烟气温,稳燃效果十分明显,但由于我国动力用煤普遍存在煤质较差且煤种多变的特点,约有半数动力用煤在不同程度上属于易结渣类型煤种^[4],同时由于卫燃带处于炉内高温区且表面比较粗糙,因此极易引起煤灰在其表面产生结渣^[5-7]。

锅炉运行时有诸多因素会影响卫燃带表面结渣,其中煤灰的化学成份特性具有重要影响。Fe₂O₃ 是煤灰重要的组成成份,在煤灰中含量变化范围较大,一般在 1% ~ 45% 之间,个别煤种甚至可达 60% 以上^[8]。煤灰中的 Fe₂O₃ 对煤灰熔融特性的影响主要与环境气氛有关^[9]: 在弱还原性气氛下,Fe₂O₃ 会被还原为 FeO,使煤灰熔融温度迅速降低,且由于 FeO 很容易与灰渣中的 CaO、SiO₂ 及 Al₂O₃ 等物质反应形成低熔点共熔体,因而具有显著的助熔效果; 在氧化性气氛中,由于 Fe³⁺ 离子具有很高的极性,是聚合物的构成者,因此可显著提高煤灰熔融性温度^[10]。本研究拟通过静态煅烧试验来说明煤灰中 Fe₂O₃ 含量的变化对其熔融特性及其在卫燃带耐火材料表面结渣特性的影响,对燃煤锅炉卫燃带的合理选用及设计具有现实的指导意义。

1 试 验

1.1 试验灰样的制备及分析

试验用煤为冷水江页岩煤,首先根据 GB/T1574 - 1995 规定将其进行标准灰化,然后磨制成粒径为 75 μm(过 200 目筛)的煤灰试样。采用 GKF - III 型硅酸盐快速成份分析仪得到试验煤灰化学成份,如表 1 所示。

表 1 试验煤灰的化学成份(%)

Tab. 1 Chemical composition of the coal - produced ash under the test(%)

灰样	煤灰化学成份							
	SiO ₂	Al ₂ O ₃	Fe ₂ O ₃	TiO ₂	CaO	MgO	K ₂ O	Na ₂ O
冷水江页岩煤灰	61.00	33.21	1.53	0.38	0.62	0.82	1.90	0.54

为了分析煤灰中 Fe₂O₃ 含量渐变对其熔融特性及结渣性的影响,依次向冷水江页岩煤灰中加入不同质量的粒径为 75 μm 的 Fe₂O₃ 粉末,制得 Fe₂O₃

含量分别为 1.53% (冷水江页岩煤基灰)、10%、20%、30%、40% 的煤灰试样若干,并将所配备的煤灰试样封装后置于振动仪上在 10 kHz 频率下振动 5

收稿日期: 2013 - 02 - 27; 修订日期: 2013 - 06 - 24

作者简介: 陈冬林(1963 -),男,湖南石门人,长沙理工大学教授,博士。

min, 使加入的 Fe₂O₃ 粉末与冷水江页岩煤灰充分均匀混合。

1.2 卫燃带耐火材料板的制备

试验用卫燃带耐火材料板为电站锅炉卫燃带常采用的刚玉质及碳化硅质耐火材料板, 考虑到 Cr₂O₃ 具有较好的抗渣性能, 因此在卫燃带耐火材料板的制备过程中均加入了少量的 Cr₂O₃。试验用卫燃带耐火材料板配方组成如表 2 和表 3 所示。其中根据 Al₂O₃ 含量的不同, 将刚玉质耐火材料分为高铝刚玉板(Al₂O₃ = 87%) 及中铝刚玉板(Al₂O₃ = 77%) 两种。

表 2 高铝与中铝刚玉质耐火材料板配方组成(%)

Tab. 2 Formulae composition of the high aluminum and low aluminum corundum refractory plate(%)

材料板	材料板成份					
	36 号白刚玉	15 号白刚玉	α - Al ₂ O ₃	Cr ₂ O ₃	ZrSiO ₄	CMC
高铝刚玉板	40	17	30	5	5	3
中铝刚玉板	40	7	30	15	5	3

表 3 碳化硅质耐火材料板配方组成(%)

Tab. 3 Formulae composition of the silicon carbide refractory plate(%)

	61 μm SiC	120 μm SiC	Al ₂ O ₃	Cr ₂ O ₃	ZrSiO ₄	CMC	木质素
含量	38	29	15	10	4.8	0.2	3

将原料按照表 2 及表 3 所示百分比配料完成后, 在 20 MPa 油压机上制成 50 mm × 50 mm × 5 mm 的试样, 待试样烘干后在还原性气氛(2% ~ 4% CO) 硅钼棒炉中于 1 500℃ 下煅烧 5 h。

1.3 试验过程

将制备得到的煤灰试样分为两部分, 一部分经糊精溶液润湿后, 使用灰锥模将其压制制成三角锥体, 在空气中风干后置于 SDAF2000b 灰熔融性测试仪内测出不同 Fe₂O₃ 含量煤灰的熔融特性温度。

另一部分则以相同的面积及厚度均匀疏松的散布在 3 种卫燃带耐火材料板表面, 即制成 15 个煤灰/耐火材料板试样, 制备时应注意避免煤灰受压而致密化, 待煤灰/耐火材料板试样制备完成后, 将其依次置入硅钼棒高温马弗炉中进行煅烧。设定马弗

炉的升温程序为: 首先将其由室温 20℃ 按照 5 ℃ / min 的升温速率加热至 800 ℃, 再按照 10 ℃ / min 的升温速率加热至 1 350 ℃ 时, 当炉温达到 1 350 ℃ 时, 保温运行 40 h。在煅烧过程中, 为保持炉内弱氧化性气氛, 采用非密闭加热方式, 即关闭炉门时留有少许缝隙, 使空气能够进入炉内, 从而保证煅烧过程中充足的氧气。煅烧完成后, 待煤灰/耐火材料板试样在炉内自然冷却至室温后取出, 观察煤灰在卫燃带耐火材料板表面的结渣情况, 并对煤灰渣进行 X 射线衍射(XRD) 分析。

2 试验结果分析

2.1 Fe₂O₃ 含量渐变对煤灰熔融特性的影响

图 1 为煤灰中 Fe₂O₃ 含量渐变对其熔融特性的影响, 由图中可以看出, 随 Fe₂O₃ 含量的逐渐增加, 表征煤灰熔融特性的 4 种温度均呈下降趋势, 并在 Fe₂O₃ 含量为 30% 时降至最小值, 此后随 Fe₂O₃ 含量的继续增加, 煤灰熔融特性温度又转而呈上升趋势。这是因为当煤灰中 Fe₂O₃ 含量增至一定值后, 煤灰特性将逐渐趋向于 Fe₂O₃ 的物化特性, 而 Fe₂O₃ 本身是一种具有较高熔点(1 565 ℃) 的矿物质, 因而使得煤灰的熔融特性温度有所升高。另外, 由图 1 中还可看出, 随煤灰中 Fe₂O₃ 含量的变化, 煤灰变形温度 DT 及软化温度 ST 变化幅度要远大于其半球温度 HT 及流动温度 FT 的变化。

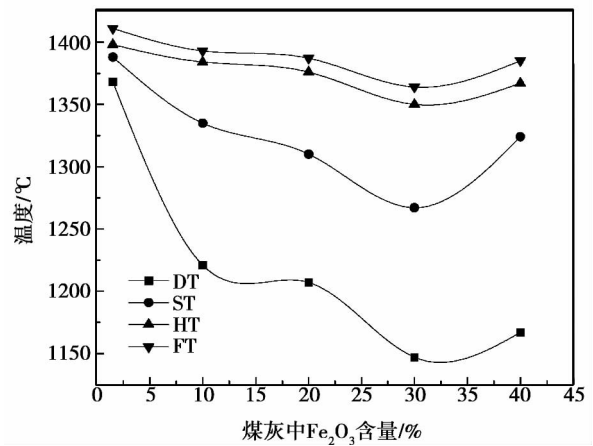


图 1 Fe₂O₃ 含量渐变对煤灰熔融特性的影响

Fig. 1 Influence of the gradual change in the Fe₂O₃ content on the fusion characteristics of coal - produced ash

2.2 试样结渣形貌分析

图 2 为不同 Fe_2O_3 含量的煤灰经 $1\ 330\ ^\circ C$ 煅烧 20 h 后在不同卫燃带耐火材料板表面的结渣形貌。由图中可以看出,随煤灰中 Fe_2O_3 含量的增加,3 种卫燃带耐火材料板表面渣样形貌均发生较大的变化,特别是当 Fe_2O_3 含量由 1.53% 增至 20% 的过程中,3 种卫燃带耐火材料板表面灰渣的颜色、残留量以及灰渣与卫燃带耐火材料板之间的粘结程度均发生明显的变化。但当 Fe_2O_3 含量由 30% 增至 40% 时,3 种卫燃带耐火材料板表面灰渣形貌不再发生

明显变化,均呈现为黑褐色,且结渣程度同样不再发生明显变化。图 2(a)、(b) 分别为不同 Fe_2O_3 含量的煤灰在高铝、中铝刚玉质耐火材料板表面的结渣形貌,由两图可知,当煤灰中 Fe_2O_3 含量相同时,两种刚玉质耐火材料板表面的结渣形貌基本相近,且随 Fe_2O_3 含量的增大,两者受灰渣侵蚀程度的变化规律也较为相似。比较表 2 两种刚玉质耐火材料板的配方组成可知,当刚玉质耐火材料中 Al_2O_3 及 Cr_2O_3 含量变化不大时,其对 Fe_2O_3 含量变化较为明显的煤灰的抗结渣性能影响不大。

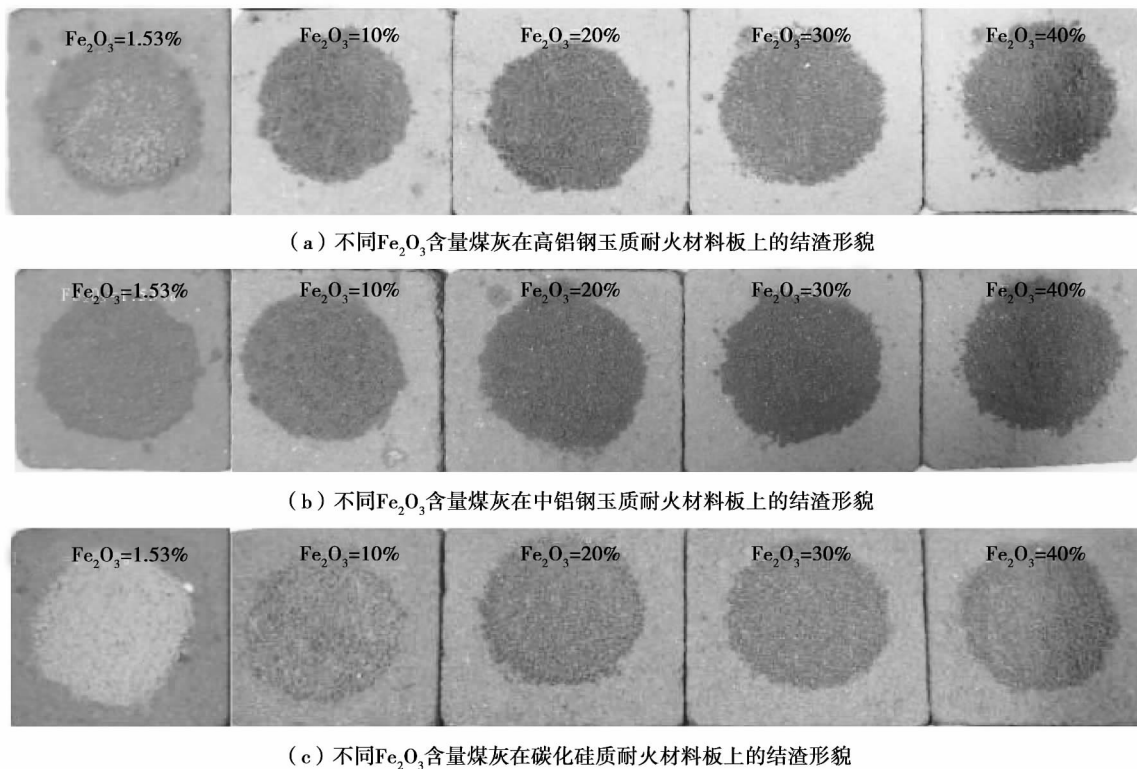


图 2 不同 Fe_2O_3 含量的煤灰在不同卫燃带耐火材料板上经 $1\ 330\ ^\circ C$ 煅烧 20 h 后的结渣形貌

Fig. 2 Slagging morphology of the coal - produced ash at various Fe_2O_3 contents after it had been calcined at $1\ 330\ ^\circ C$ for 20 hours on the refractory plate with various refractory belts

不同 Fe_2O_3 含量的煤灰在碳化硅质耐火材料板表面结渣形貌如图 2(c) 所示。由该图可知,当 Fe_2O_3 含量为 1.53% 时,由于其软化温度 ($ST = 1\ 368\ ^\circ C$) 高于试验温度,此时碳化硅耐火材料板表面的灰渣呈淡黄色,渣层分布较为疏松,与耐火材料板之间的粘结程度较低。而当 Fe_2O_3 含量增至 10%、20% 时,碳化硅耐火材料板表面灰渣则变为浅棕色与黑绿色,与耐火材料板之间的粘结也变得较

为紧密。这表明,当煤灰中 Fe_2O_3 含量由基灰的 1.53% 增至 10%、20% 时,其对碳化硅质耐火材料板的侵蚀作用将不断加剧,且在煅烧过程中与碳化硅质耐火材料板之间反应生成的产物也不断发生变化,从而致使碳化硅质耐火材料板表面灰渣形貌特征发生较大的变化。另外,由图 2(c) 还可知,当煤灰中 Fe_2O_3 含量增至 30% 以上时,碳化硅质耐火材料板表面灰渣均呈黑褐色,灰渣形貌及其与耐火材

料板之间的粘结程度随 Fe₂O₃ 含量的增加不再发生明显的变化。

分别比较 Fe₂O₃ 含量为 1.53%、40% 的灰样在 3 种卫燃带耐火材料板表面的结渣形貌发现: 当煤灰中 Fe₂O₃ 含量为 1.53% 时, 碳化硅质耐火材料板表面的灰渣相对于两种刚玉质耐火材料板表面灰渣表现的较为疏松, 与其粘结程度较为轻微。另外, 碳化硅质耐火材料板表面剩余灰渣也较多, 而两种刚玉质耐火材料板表面灰渣残余量则较少, 大部分灰渣已在煅烧过程中渗透、侵蚀至耐火材料板内部。这说明, 当煤灰中 Fe₂O₃ 含量较低时, 其在碳化硅质耐火材料板表面的结渣程度弱于其在刚玉质耐火材料板表面的结渣程度。当煤灰中 Fe₂O₃ 含量增至 40% 时, 煤灰在 3 种卫燃带耐火材料板表面的结渣程度却基本一致, 在外观形貌上基本没有出现较大的差别。由此可知, 当锅炉燃用煤灰中 Fe₂O₃ 含量较低的煤时, 采用碳化硅质耐火材料作为卫燃带使用可取得较好的抗结渣效果; 而当锅炉燃用煤灰中 Fe₂O₃ 含量较高的煤时, 采用刚玉质卫燃带与碳化

硅质卫燃带的抗结渣效果基本一致。

2.3 灰渣 XRD 分析

研究中, 为分析煤灰中 Fe₂O₃ 含量变化对其在卫燃带表面结渣特性的影响, 对碳化硅质耐火材料板表面灰渣进行 XRD 分析。碳化硅耐火材料板表面灰渣 XRD 图谱如图 3 所示。当煤灰中 Fe₂O₃ 含量为 1.53% 时, 灰渣的主要矿物质为石英及莫来石, 这两种物质均具有较好的耐高温性能及稳定的物化特性, 因而此时碳化硅质耐火材料板表面灰渣较为疏松, 结渣程度较轻。而当煤灰中 Fe₂O₃ 含量增至 10%、20% 时, 灰渣中除含有石英及莫来石外, 还出现了少量的三氧化二铬及锆英石, 如图 3(b)、(c) 所示。根据煤灰化学组分及碳化硅质耐火材料板的配料组成可知, 灰渣中的三氧化二铬及锆英石均来源于碳化硅耐火材料板, 这说明当煤灰中 Fe₂O₃ 含量增至 10%、20% 时, 在煅烧过程中, 煤灰与耐火材料板之间已经发生了较为强烈的相互渗透作用, 使得耐火材料板中矿物成分反向渗透至煤灰中, 同时这也间接说明此时煤灰对耐火材料的渗透、侵蚀作用也相应增强。

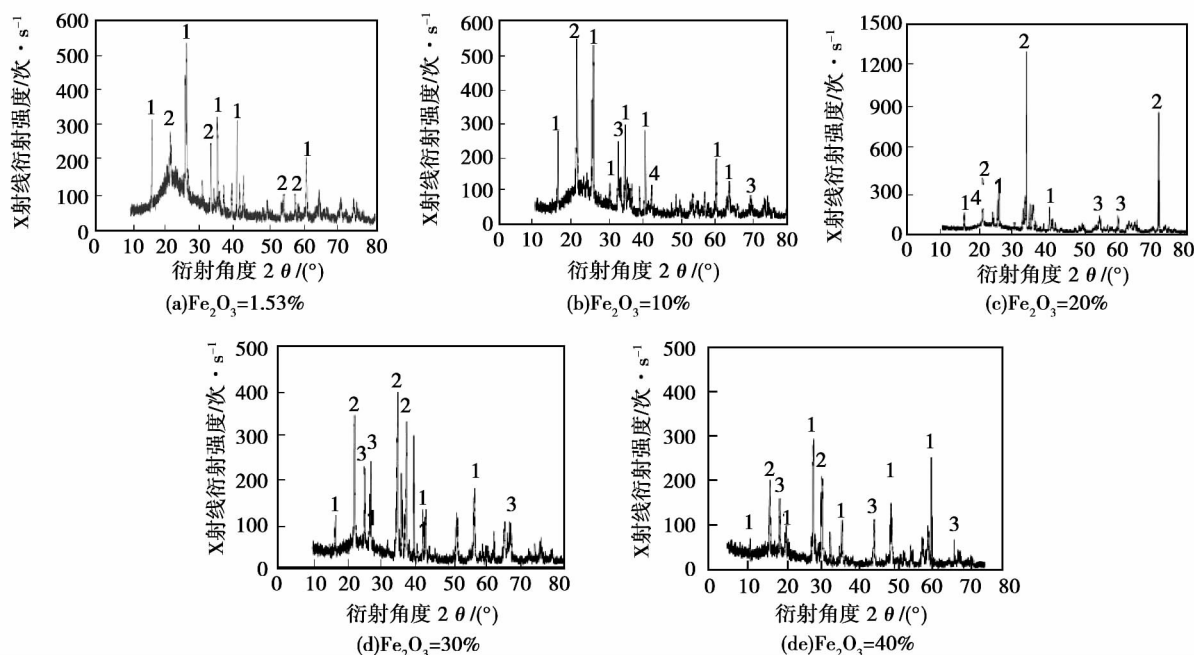


图 3 碳化硅质耐火材料板上不同 Fe₂O₃ 含量煤灰试样经 1 330 °C 煅烧 20 h 后灰渣 XRD 图谱

Fig. 3 XRD spectrum of the ash and slag after the coal - produced ash samples at various Fe₂O₃ contents had been calcined at 1 330 °C for 20 hours on the silicon carbide refractory plate

当煤灰中 Fe₂O₃ 含量增至 30%、40% 时, 灰渣

的主要矿物成份均为石英及莫来石, 还有少量三氧

化二铬,而锆英石则在灰渣中未检测到,如图 3(d)、(e)所示。由此可知,当煤灰中 Fe_2O_3 含量增至 30% 以上时,煤灰与耐火材料板之间的相互渗透作用将随 Fe_2O_3 含量的增加而有所减弱,这也说明了此时耐火材料板表面灰渣形貌变化不再明显的原因。

3 结 论

(1) 随煤灰中 Fe_2O_3 含量的增加,表征煤灰熔融特性的 4 种温度均呈现出不同程度的下降趋势,其中变形温度 DT 与软化温度 ST 下降速度最快,但当煤灰中 Fe_2O_3 含量增至一定值后,煤灰的熔融温度将随 Fe_2O_3 含量的增加反而呈上升趋势。

(2) 随着煤灰中 Fe_2O_3 含量的增加,3 种卫燃带耐火材料板表面渣样形貌均发生较大变化,且结渣程度均逐渐增强,但当 Fe_2O_3 含量增至一定值后,卫燃带耐火材料板表面结渣程度将不再明显增强,反而转呈减弱的趋势。

(3) 当锅炉燃用低 Fe_2O_3 含量的煤时,采用碳化硅质耐火材料作为卫燃带可取得较好的抗结渣效果;而当燃用 Fe_2O_3 含量较高的煤时,采用刚玉质卫燃带与碳化硅质卫燃带的抗结渣效果基本一致。

(4) 当刚玉质卫燃带中 Al_2O_3 及 Cr_2O_3 含量变化不大时,其对 Fe_2O_3 含量变化较为明显的煤灰的抗结渣性能影响不大。

参考文献:

- [1] CHEN D L, ZHENG C G. Quasi-constant temperature combustion for improving overall performance of a coal-fired boiler[J]. *Combustion and Flame* 2003, 134(1/2): 81-92.
- [2] 谭旦辉,陈冬林,张英才. 煤粉锅炉卫燃带的数值模拟[J]. 长沙理工大学学报(自然科学版) 2011, 8(3): 61-65.
TAN Dan-hui, CHEN Dong-lin, ZHANG Ying-cai. Numerical simulation of the refractory belts of a pulverized coal-fired boiler[J]. *Journal of Changsha University of Science and Technology(Natural Science)* 2011, 8(3): 61-65.
- [3] 陈冬林,陈彦菲,鄢晓忠,等. 环境气氛对煤灰在 $\text{Al}_2\text{O}_3\text{-Cr}_2\text{O}_3\text{-ZrO}_2$ 材料上结渣的影响[J]. *耐火材料*, 2008, 42(5): 368-371.
CHEN Dong-lin, CHEN Yan-fei, YAN Xiao-zhong, et al. Effect of the ambient atmosphere on the slagging of the coal ash on $\text{Al}_2\text{O}_3\text{-Cr}_2\text{O}_3\text{-ZrO}_2$ material [J]. *Refractory Materials* 2008, 42(5): 368-371.
- [4] 袁颖,相大光,姚伟. 大型锅炉炉膛结渣的预防[J]. *中国电力*, 1994(7): 2-7.
YUAN Ying, XIANG Da-guang, YAO Wei. Prevention of the slagging in the furnace of a large-sized boiler [J]. *China Electric Power*, 1994(7): 2-7.
- [5] Chen F C, Bernard B A, William E L. Prediction of the effect of additives on slag resistance of $\text{Al}_2\text{O}_3\text{-SiO}_2\text{-C}$ bond phase in air [J]. *Calphad* 2003, 27(1): 115-125.
- [6] 周俊虎,赵晓辉,刘建中,等. 锅炉内卫燃带上高熔点灰渣沉积机理分析[J]. *中国电机工程学报* 2008, 28(14): 20-26.
ZHOU Jun-hu, ZHAO Xiao-hui, LIU Jian-zhong, et al. Analysis of the mechanism governing the deposition of the ash and slag at a high melting point on the refractory belts in a boiler [J]. *Proceedings of China Electric Machinery Engineering* 2008, 28(14): 20-26.
- [7] 何金桥,鄢晓忠,陈冬林. 燃煤锅炉碳化硅质卫燃带表面结渣行为[J]. *动力工程学报* 2011, 31(9): 659-663.
HE Jin-qiao, YAN Xiao-zhong, CHEN Dong-lin. Slagging behavior on the surface of carborundum-based refractory belts in a coal-fired boiler [J]. *Journal of Power Engineering* 2011, 31(9): 659-663.
- [8] 潘攀. 煤的结渣特性研究[D]. 保定: 华北电力大学, 2006.
PAN Pan. Study of the slagging characteristics of coal [D]. Baoding: North China University of Electric Power, 2006.
- [9] Vorres K S. Prediction of ash melting behaviour from coal Ash Compositions [J]. *Trans ASME J Eng Power*, 1979, 101: 497-503.
- [10] 戴爱军,杜彦学,谢欣馨. 煤灰成分与灰熔融性关系研究进展[J]. *煤化工* 2009(4): 16-19.
DAI Ai-jun, DU Yan-xue, XIE Xin-xin. Advances in the study of the relationship between the coal ash composition and ash melting property [J]. *Coal Chemical Industry* 2009(4): 16-19.

(陈滨 编辑)

shows that the mean deviation of the flue gas temperature obtained by using the model in question is 6.28% and the mean deviation of the cooling water temperature is 9.45%. The foregoing can offer reference for designing high efficiency heat exchangers. **Key words:** condensation heat exchange ,natural gas-fired boiler ,pumping action

基于 CFD 技术的多级离心泵汽蚀性能研究 = Study of the Cavitation Performance of a Multi-stage Centrifugal Pump Based on the CFD Technology [刊 汉] CHEN Fang-fang ,LI Zhi-peng ,WANG Chang-sheng(College of Energy Source and Power Engineering ,Changsha University of Science and Technology ,Changsha ,China ,Post Code: 410114) //Journal of Engineering for Thermal Energy & Power. -2013 28(5) . -514 ~ 517

To enhance the cavitation-resistant performance of a multi-stage pump ,the first-stage impeller structure was improved and designed with the inlet diameter and outlet width of the impeller being increased ,making the leading edge of the blades extended towards the inlet direction ,the curvature radius of the covering plate in the inlet part increased ,thickness of the blades at the inlet decreased ,the diameter of the water suction chamber at the inlet increased accordingly and the annulus space of the water suction chamber expanded. By using the software Fluent ,the flow field inside the first-stage impeller was numerically simulated before and after the improvement. The simulation results show that the area where cavitation phenomena take place is located on the back of the impeller close to the rim and after the improvement ,the flow is smooth and stable in the flow path of the first-stage impeller with the pressure and speed distribution being uniform. By adopting the numerical simulation method ,the cavitation performance of the pump was predicted before and after the improvement and verified by a cavitation test. The relative errors are 2.6% and 2.5% respectively. The cavitation allowance decreases after the improvement and is less than the value stipulated and the cavitation performance is improved ,achieving the improvement goals. The numerical simulation results can provide reliable underlying bases for design and improvement of multi-stage pumps. **Key words:** multi-stage centrifugal pump ,first-stage impeller ,cavitation performance ,CFD

煤灰中 Fe_2O_3 含量对卫燃带表面结渣的影响 = Influence of the Fe_2O_3 Content of Coal Ash on the Slagging on the Surface of the Refractory Belt [刊 汉] CHEN Dong-lin ,DU Yang ,CHEN Wen-wei ,et al(College of Energy Source and Power Engineering ,Changsha University of Science and Technology ,Changsha ,China ,Post Code: 410076) //Journal of Engineering for Thermal Energy & Power. -2013 28(5) . -518 ~ 522

With Lengshuijiang River-originated shale coal ash serving as the base ash , Fe_2O_3 powder in various weights was

added to prepare several coal ash samples with the Fe_2O_3 powder content being 1.53% ,10% ,20% ,30% and 40% respectively. Firstly ,the pyramid method was adopted to measure the influence of the changes of the Fe_2O_3 powder content on the melting characteristics of coal ash. Afterwards ,the coal ash with different Fe_2O_3 powder contents was laid uniformly and loosely on the surface of the refractory belt plates made from silicon carbide ,high alumina corundum and medium aluminum corundum respectively and placed into a high temperature muffle furnace to calcine for 40 hours at 1 330 °C. Upon the completion of the calcination ,the slagging characteristics of the three kinds of the refractory belt plates were observed and an X-ray diffraction analysis was performed of the coal ash. The test results show that with an increase of the Fe_2O_3 powder content of the coal ash ,all the melting temperatures of the coal ash assume a descending tendency and at the same time ,the slagging extents on the surface of the plates tend to be worsened. However ,when the Fe_2O_3 powder content of the coal ash increases to a given value ,their melting temperatures assume an ascending tendency instead and the slagging extents on the surface of the plates will no longer get increased but somewhat decreased. **Key words:** coal ash ,refractory belt ,melting characteristics ,slagging , Fe_2O_3 Powder

平直斜翅管表面碳酸钙污垢初始阶段结垢特性 = **Fouling Characteristics of the CaCO_3 Foul on the Surface of a Straight and Obliquely-finned Tube in the Initial Stage** [刊 ,汉] ZHAO Ping ,SHENG Jian ,ZHANG Hua (College of Energy Source and Power Engineering ,Shanghai University of Science and Technology ,Shanghai ,China ,Post Code: 200093) //Journal of Engineering for Thermal Energy & Power. -2013 28(5) . -523 ~528

A dynamic fouling test was performed of a bare tube and a straight and obliquely-finned tube at different CaCO_3 concentrations and flow speeds to obtain the influence of the CaCO_3 concentration ,flow speed and straight and obliquely-finned tube on the CaCO_3 crystal precipitation fouling process. It has been found that to increase the concentration can make both homogeneous nucleation speed and crystal nucleus growth speed increased and both foul crystal particle concentration on the boundary surface of the solution for heat exchange and foul ion concentration increased. The former makes more foul adsorbed on the heat exchange surfaces and the latter forces the heterogeneous nucleation speed and growth speed increased. To increase the flow speed can make the crystal nuclei and foul crystal formed on the surface of the bare tube and foul heat resistance decreased but the induction period extended and force the initial nucleation of the straight and obliquely-finned tube increased but the induction period extended and the foul quantity and heat resistance decreased. The straight and obliquely-finned tube has a bigger total heat exchange coefficient and a smaller foul heat resistance than the bare tube albeit the foul quantity is slightly more. **Key**